JOURNAL OF MATERIALS SCIENCE 31 (1996) 246–251

Melt spinning as a microstructural analogue for aluminide diffusion coating

W. F. GALE, R. V. NEMANI
Materials Engineering Program, Auburn University, AL 36849, USA
P. SCHUMACHER
Department of Materials Science and Metallurgy, University of Cambridge, Cambridge, CB2 3QZ, UK

The feasibility of using melt spinning, of a high alloy nickel aluminide, as a microstructural analogue for aluminide diffusion coated nickel base superalloys is investigated in this paper. Transmission electron microscopy studies are used to characterize the relationship between coating and melt spun analogue microstructures. Attention is focused on three phases that are of principal importance in coating mechanical properties, namely: the B2 type β phase coating matrix, $L1_2$ type γ′ precipitates and $M_{23}X_6$ carbides.

The microstructure of the β matrix of the melt spun analogue is shown to closely resemble that of the coating. Evidence is presented that the formation of γ′ in the melt spun alloy generally occurs in a similar manner to that in the coating. The formation of $M_{23}X_6$ in close association with γ′ in the melt spun materials is compared to similar events in the coatings. Limitations in the ability of the melt spun materials to recreate the microstructures resulting from incorporation of substrate $M_{23}X_6$ into the coating and formation of $M_{23}X_6$ within β precursor phases are discussed.

1. Introduction

Pack aluminide diffusion coating is a common method of protecting nickel base superalloys against high temperature oxidative attack in applications such as aero gas turbine blades [1]. Pack aluminide coatings are formed by reaction between nickel emanating from the component to be coated and aluminium supplied by the pack [2]. Nominally, the coatings are composed of a B2 type intermetallic compound (denoted conventionally as β) with a nominal composition of NiAl [3]. In practice, however, the chemistry and microstructure of coatings produced on commercial superalloys are complex and evolve during elevated temperature service [4, 5].

Although pack aluminization offers a marked increase in the oxidation resistance of superalloys, this is obtained at the expense of the fatigue resistance of the coated system [6]. As a result, coatings must be included in component lifing strategies and this requires a detailed knowledge of coating mechanical properties. Data on the mechanical properties of the overall coating can be obtained by conducting mechanical testing of aluminized superalloys in the bulk [7] or thin foil form [8]. However, testing of the entire coating and substrate system does not provide opportunities for obtaining mechanical properties information for selected regions of the complex coating microstructures. Hence, the ability to produce mechanical test specimens with a microstructure analogous to a single region of a given coating would greatly increase the range of available mechanical properties data.

In this paper, the use of melt spun foils of a high alloy nickel aluminide is examined as a practicable approach for the preparation of microstructural analogues for individual microstructural regions of aluminide diffusion coatings.

2. Experimental procedure

Melt spun foils were prepared by induction remelting of an arc melted precursor (having the composition shown in Table I) in a boron nitride crucible and ejecting the melt onto a copper wheel rotating at a speed of approximately 30 $m\,s^{-1}$. Argon was used both as the atmosphere for the melt spinning process and to achieve ejection of the melt. Melt spinning resulted in ribbons with a thickness of approximately 50 μm and a width of around 4 mm.

The melt spun ribbons were examined in both the as-spun condition and after ageing at 850 °C in a 10^{-5} mPa vacuum for up to 16 h. Samples were characterized using both a Jeol 1200EX transmission electron microscope (TEM) operating at 120 kV and a Jeol 840 scanning electron microscope (SEM) operating at 20 kV. In both cases analytical information was obtained using ultrathin window energy dispersive X-ray spectroscopy (EDS) with a Tracor-Northern 5500 analyser. Details of SEM and TEM specimen preparation procedures may be found elsewhere [4].

0022–2461

TABLE I Nominal composition of the melt spun material

Element	Content (wt %)
Ni	60.0
Co	13.0
Al	12.0
Cr	8.0
Ti	3.1
Mo	1.6
V	1.0
W	1.0
C	0.3

3. Results

In this section, microstructural development in the melt spun alloy will be described for both the as-melt spun and heat treated conditions.

3.1. As-melt spun ribbon

The microstructure of the as-melt spun material was found to consist of a B2 type β phase matrix (Figs 1 and 2). The β phase was roughly equiaxed with a grain size of around 3–5 μm and was strongly enriched in nickel compared to aluminium. The β phase showed the tweed contrast and diffraction anomalies that are characteristic of this B2 compound. Despite the nickel enrichment of the β phase, no evidence was found for the formation of 7R or 3R type β derivatives [9, 10].

The β phase matrix of the as-spun material was found to contain extensive deposits of an $L1_2$ type γ′ phase (Figs 1 and 2). Apart from having a lower aluminium content, the γ′ was compositionally similar to β. The γ′ deposits adopted two characteristic morphologies, namely:

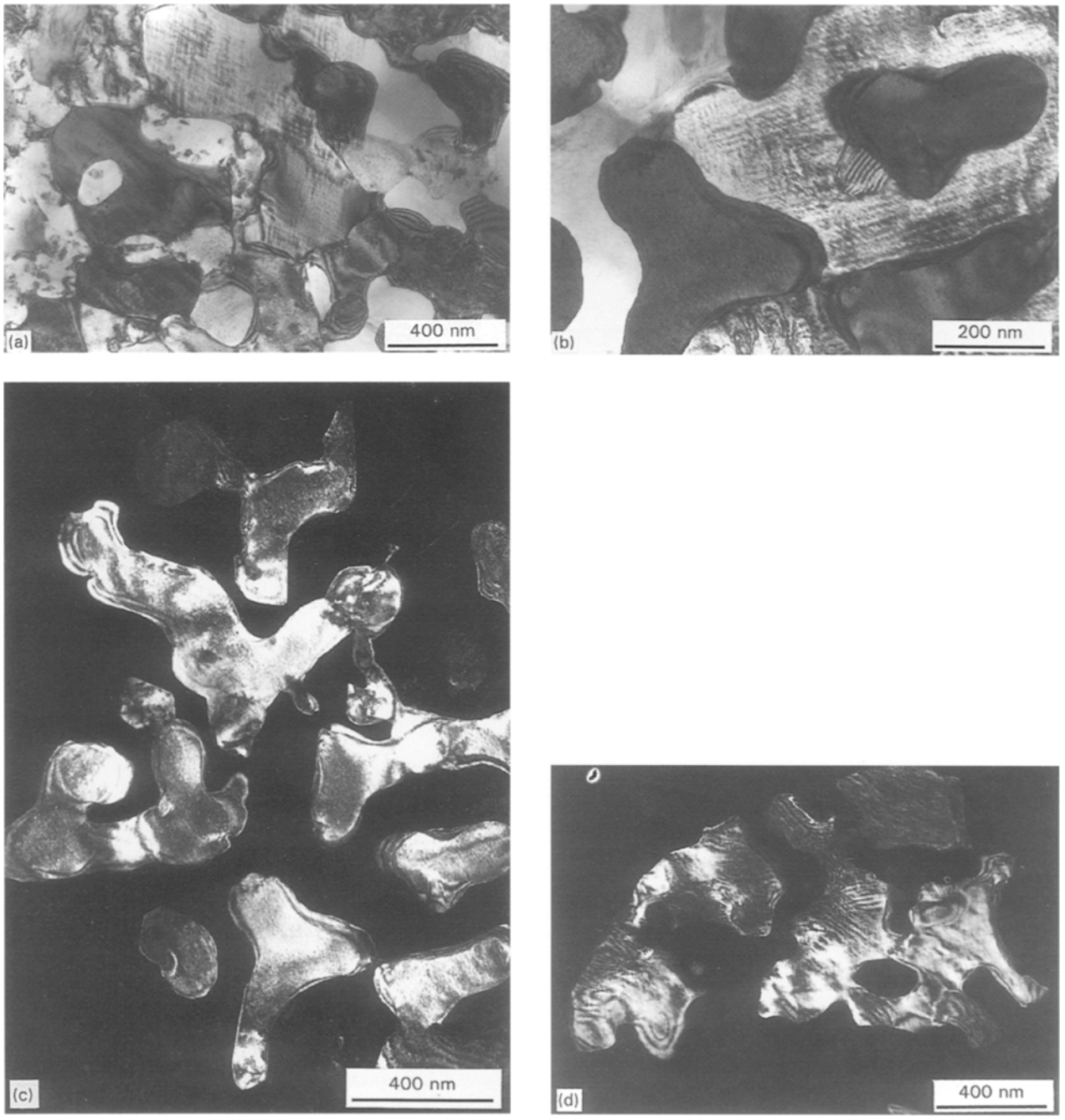

Figure 1 Character of the β and γ′ phases in the as-melt spun condition. Bright field images of (a) general microstructure, and (b) type II γ′ deposits (dark) in β phase (light). Dark field images of (c) type II γ′ deposits [operating reflection, $g = (2\,0\,0)_{\gamma'}$], and (d) β phase surrounding type II γ′ deposits [$g = (1\,\bar{1}\,0)_{\beta}$].

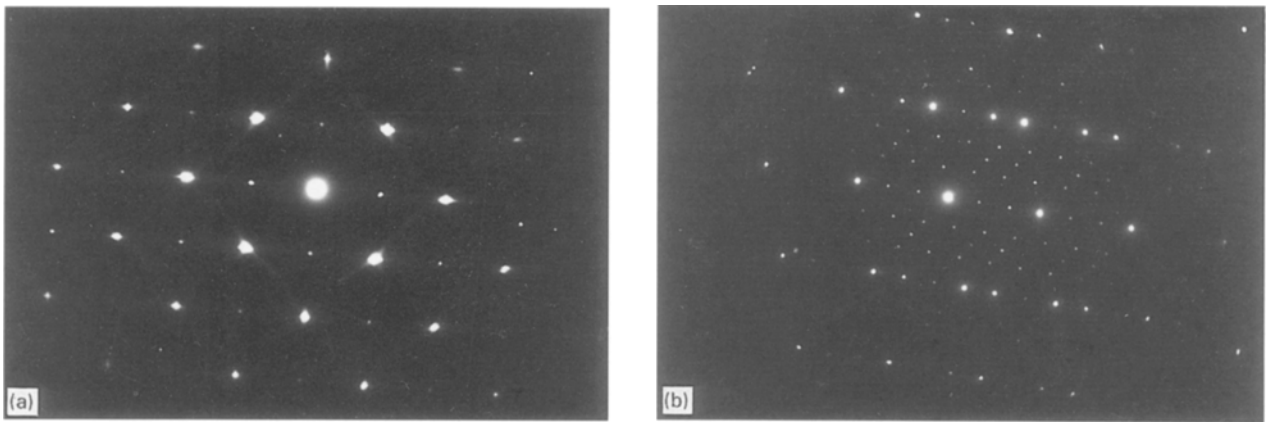

Figure 2 Selected area diffraction patterns showing the crystallography of the β, γ′ and $M_{23}X_6$ phases for beam direction, *B*, equal to (a) $[1\,0\,0]_\beta$ (sample aged for 2 h at 850 °C), and (b) $[1\,1\,0]_{\gamma'/M_{23}X_6}$ showing a twinned γ′ precipitate with one of the twin variants forming a cube–cube orientation relationship with an $M_{23}X_6$ precipitate (sample aged for 16 h at 850 °C).

1. Type I: ellipsoidal precipitates (around 200–500 nm long and 50–200 nm wide) usually with a single midrib twin plane (although some multiple twinning was observed). These formed intragranularly within the β phase, often as interlinked networks of precipitates aligned along $\langle 1\,2\,0\rangle_{\gamma'}$ directions. The formation of twinned γ′ precipitates on β–β boundaries was also noted.

2. Type II: irregularly shaped, often coalesced, precipitates with a wide range of sizes (typically from around 200 nm to 1 μm). This morphology was associated with precipitation both intragranularly within the β phase and on β–β boundaries. The extent of this γ′ formation was found to vary markedly from region to region (and in some places γ′ constituted the major phase).

In both cases a Kurdjumov–Sachs type orientation relationship was produced between the β and γ′ phases such that

$$[1\,1\,1]_\beta // [1\,1\,0]_{\gamma'}$$

$$(\bar{1}\,1\,0)_\beta // (1\,\bar{1}\,1)_{\gamma'}$$

Although the as-spun foils were predominantly composed of β and γ′, regions of disordered Al type γ phase were also observed. These were similar (in terms of morphology and orientation relationship with β) to the type II γ′ deposits.

3.2. 850 °C aged ribbon

Ageing of the melt spun foil at 850 °C was found to result in significant modification of the as-spun microstructure. Ordering of the γ deposits to γ′ was found to occur during ageing. Significant ordering was observed after 2 h at 850 °C, resulting in the formation (Fig. 3) of cuboidal γ′ precipitates (generally around 50–200 nm on edge) within the γ deposits. These γ′ precipitates aligned along $\{1\,0\,0\}_\gamma$ in the conventional manner. Following 16 h ageing at 850 °C, ordering of the γ deposits to γ′ was completed. Simultaneously with the ordering of γ to γ′, fresh γ′ was precipitated from the β phase, Most of the new γ′ precipitated from the β phase had a type I morphology, although a limited number of type II morphology precipitates were also observed. The γ′ precipitated from β during ageing could be readily distinguished from other γ′ deposits due to the formation of a different orientation relationship with the β phase. This orientation relationship was of the Nishiyama–Wasserman type, such that

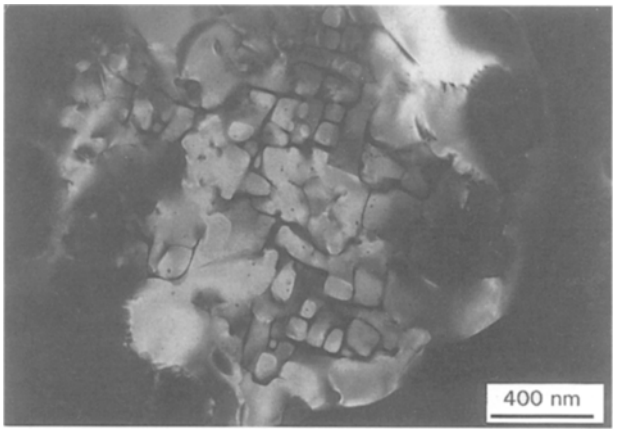

Figure 3 Local ordering of γ (originating from the as-melt spun condition) to γ′ after 2 h ageing at 850 °C, dark field with operating reflection, $g = (1\,1\,0)_{\gamma'}$.

$$[0\,0\,1]_\beta // [1\,1\,0]_{\gamma'}$$

$$(1\,\bar{1}\,0)_\beta // (\bar{1}\,1\,1)_{\gamma'}$$

Ageing was found to coarsen the existing type I γ′ deposits, principally by broadening of the precipitates to a relatively equiaxed morphology.

In the as-spun condition, no carbide phases were observed in the ribbons, howevers, extensive precipitation of $M_{23}X_6$ (for which *M* was predominantly chromium with some molybdenum and *X* was carbon) was observed after 850 °C ageing. $M_{23}X_6$ always formed in association with γ′ precipitates (an example of this type of precipitation is shown in Fig. 4). Both the original γ′ present after melt spinning and the new γ′ produced as a result of ageing served as sites for precipitation of $M_{23}X_6$. The $M_{23}X_6$ and γ′ phases were cube–cube orientation related (Fig. 2b). The

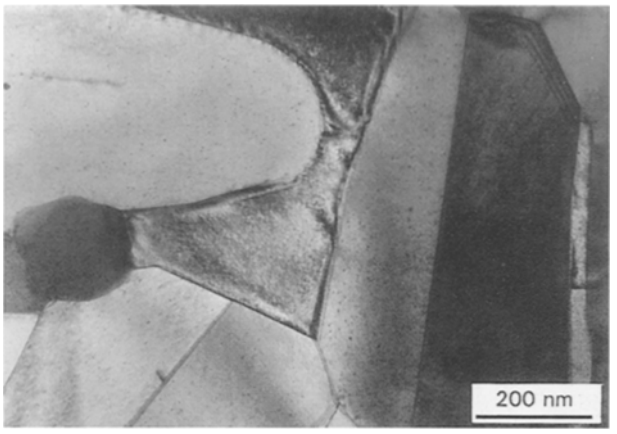

Figure 4 $M_{23}X_6$ precipitated in association with ellipsoidal twinned type I γ' deposits in a sample aged for 2 h at 850 °C.

main site for formation of $M_{23}X_6$ was found to be β–γ' interfaces. In general, growth of the $M_{23}X_6$ took place into the β phase, although growth into the γ' was also observed. Some $M_{23}X_6$ precipitation also took place intragranularly within the γ'. In all cases, $M_{23}X_6$ formed roughly equiaxed polygonal precipitates with diameters in the 100–500 nm range.

4. Discussion

The composition of the melt spun material was based on previous studies by one of the authors [4, 5] of the microstructure of high activity aluminide diffusion coatings on a single crystal nickel base superalloy with principal alloying additions of Co, Cr, Al, Ti, Mo and V. In these studies four basic microstructural layers were identified in the coatings, namely:

1. oxide: Al_2O_3 on the coating surface,
2. coating surface layer: β phase matrix plus γ' precipitates,
3. main coating layer: β phase matrix plus (predominantly) $M_{23}X_6$ precipitates, and
4. coating transitional layer: β phase matrix plus (predominantly) γ' and $M_{23}X_6$ precipitates.

Unless indicated otherwise, the coatings considered in this discussion are in either the as-alloy aged condition, i.e. pack aluminized at 870 °C for 4 h, diffusion treated at 1100 °C for 1 h and aged at 870 °C for 16 h, or have received an additional thermal exposure of up to 140 h at 850 °C in air or a 10^{-2} Pa vacuum.

The composition of the melt spun material was based on a region of the coating transitional layer located close to the interface with the main layer (for a 40 μm total coating thickness this region is located approximately 10 μm from the substrate). This region is rich in γ' both in the form of intra and intergranular precipitates and was chosen for use in the present investigation in the light of the large potential significance of γ' precipitation for coating mechanical properties. A comparison will now be drawn between the microstructure of the selected region of the coating [4, 5] and the melt spun materials.

The character of the β matrix of the melt spun material was similar to that of the coating. In both cases, a grain size of around 3–5 μm was observed. The high cooling rate employed in the melt spinning suppressed dendrite formation and the equiaxed morphology of the β phase was similar to that observed in the coatings. Generally similar compositions were noted for the β phase after 16 h 850 °C ageing for the melt spun material and 138 h 850 °C ageing for the coatings. In both cases, the β phase was strongly enriched in nickel compared to aluminium, but no evidence was encountered of the formation of β derivatives (such as 7R or 3R martensites [9, 10]).

γ' precipitation in the melt spun material was found to be generally similar to that in coatings subjected to 850 °C exposure. In both cases, ellipsoidal (type I) γ' precipitates aligned along $\langle 1\,2\,0\rangle_{\gamma'}$ directions were observed. Both the coatings and the as-melt spun material showed Kurdjumov–Sachs type orientation relationships between β and γ'. In contrast, no evidence was found in the coatings for the formation of Nishiyama–Wasserman type orientation relationships between β and γ', as was observed in the aged melt spun material. No explanation has been found for this change in orientation relationship between the as-melt spun and aged material. However, it is noted that the two orientation relationships are closely related and have both been observed for bulk two phase β–γ' materials [11]. The irregular (type II) γ' morphology observed in the melt spun material was also noted to some extent in 850 °C exposed coatings. However, this morphology was more characteristic of coatings exposed at 1100 °C.

The ellipsoidal type I γ' precipitates were observed to be twinned in both the coatings and in the melt spun materials. In the present work, the type I precipitates were usually found to possess a single central midrib twin plane, which is characteristic of γ' precipitated in β [11]. A similar morphology was observed in the coatings for cases where single γ' precipitates formed in isolation directly from the β phase. More typically, however, the γ' precipitates formed in the coatings were found to possess multiple twins.

The predominant occurrence of multiple twinning of γ' formed in the coatings and single midrib twins for γ' formed in the melt spun material can be traced to differences in the mechanism of formation of the γ' precipitates. In the coatings, γ' and $M_{23}X_6$ formed networks of interlinked precipitates. These networks generally formed by the nucleation of γ' on an $M_{23}X_6$ precipitate. This was followed by further nucleation of γ' and/or $M_{23}X_6$ and so on. These multiple precipitation events occurred in close spatial association and frequently resulted in coalescence of γ' precipitates with different variations of the γ'–β orientation relationship and hence the formation of multiple twins. In contrast, with the melt spun samples, $M_{23}X_6$ was only precipitated after much of the γ' had already formed. In these circumstances the $M_{23}X_6$–γ' networks observed in the melt spun material were often formed as a result of bridging of the gaps between existing γ' precipitates by new $M_{23}X_6$ precipitates. Hence, γ' coalescence and the resulting formation of multiple twins was less common in the melt spun samples than for the coatings.

$M_{23}X_6$ precipitation in the aged melt spun material frequently took the form of either equiaxed polygonal

or equiaxed globular morphologies. In the coatings, equiaxed globular precipitates were most commonly produced. Comparing aged coatings and the aged melt spun materials, similar $M_{23}X_6$ precipitate sizes were observed (generally in the range 100–500 nm). In addition to the relatively fine $M_{23}X_6$ discussed above, the coating region on which the compositions of the melt spun materials were based also contained a limited number of relatively coarse (typically 500–700 nm) $M_{23}X_6$ precipitates formed during coating and diffusion treatments. These coarser precipitates were not, in general, reproduced in the aged melt spun material.

In the coatings, a range of orientation relationships were observed between $M_{23}X_6$ and other phases in the coating. The occurrence of these orientation relationships was dependent upon the manner in which $M_{23}X_6$ formed, as follows:

1. $M_{23}X_6$ precipitated during the coating and diffusion treatments, when coating matrix phases other than β were present, did not show an orientation relationship to any of the phases present in the final coating. These $M_{23}X_6$ precipitates were uncommon in the region of the coating which the melt spun material is intended to simulate.

2. The incorporation of substrate $M_{23}X_6$ precipitates into the coating (during coating formation) resulted in $M_{23}X_6$ precipitates that were cube–cube orientation related to the substrate γ–γ′. These were not orientation related to the coating matrix since no orientation relationship was observed between the single crystal substrate and the polycrystalline coating. Given the low carbon content of single crystal superalloys, numerous substrate carbide phases were not produced. Hence, incorporation of substrate carbides into the coating was an infrequent event. However, the incorporation process was more widespread than the precipitation of $M_{23}X_6$ from β precursor phases.

3. $M_{23}X_6$ precipitated in association with γ′ during (850 °C) ageing treatments was cube–cube orientation related to the γ′. This was found to be by far the commonest $M_{23}X_6$ precipitation mode in the region of the coatings selected for simulation.

$M_{23}X_6$ precipitated in the aged melt spun material almost invariably formed in association with γ′ and was cube–cube orientation related to the γ′ phase. Thus, the aged melt spun materials were able to reproduce the commonest $M_{23}X_6$ orientation relationship observed in the coatings. Furthermore, the overall microstructure of the $M_{23}X_6$ plus γ′ colonies was generally similar in the coatings and the melt spun samples. It should be noted that the $M_{23}X_6$ plus γ′ colonies formed by different routes in the melt spun foils and coatings (despite the microstructural similarity of the colonies). In the coatings the $M_{23}X_6$ plus γ′ formed in direct association, whereas in the melt spun samples, $M_{23}X_6$ often formed on pre-existing γ′ precipitates.

In contrast to the success of reproducing $M_{23}X_6$ plus γ′ colonies, the melt spun materials were unable to duplicate the remaining two $M_{23}X_6$ precipitation processes observed in the coatings. This failure is unsurprising given that the melt spun samples solidified directly into the β phase and had no equivalent to incorporation of carbides from an external source.

Apart from the formation of $M_{23}X_6$ chromium bearing phases were not observed in the melt spun material. This contrasts with the coatings for which the formation of α-Cr and other Cr–Mo phases was a noticeable feature. In the case of coatings formed on low carbon single crystal substrates, the formation of α-Cr was correlatable with depletion of the available carbon supply by the precipitation of the carbon rich $M_{23}X_6$ phase. Duplication of this effect in the melt spun materials presumably requires a reduced carbon content.

Initial *in situ* investigations of coating fracture behaviour [7] suggest that, although the analogues are only able to reproduce the formation of β, γ′ and $M_{23}X_6$ these three phases represent those that are of greatest importance for the mechanical performance of the coated superalloy system on which the melt spun analogue was based.

5. Conclusions

Melt spinning has been investigated as a route for the production of freestanding microstructural analogues for aluminide diffusion coatings on nickel base superalloys. Melt spinning was generally able to reproduce the main features of coating microstructures, however, some detailed differences were observed. As a result of the investigation, the following specific conclusions have been drawn.

1. The melt spun materials successfully duplicated the character of the β phase matrix of the coatings in terms of morphology, composition and grain size.

2. Precipitation of γ′ in the as-melt spun coatings invariably occurred with a Kurdjumov–Sachs orientation relationship to the β phase and this matched the orientation relationship observed in the coatings. Two γ′ morphologies were observed, namely: ellipsoidal precipitates with a central midrib twin plane and irregular deposits often produced by the coalescence of a number of precipitates. Both of these morphologies were characteristic of those observed in coatings. However, the irregular morphology was generally observed in coatings aged at higher temperatures (1100 °C) than for those exhibiting the ellipsoidal morphology (850–950 °C).

3. γ′ precipitated during ageing of the melt spun foils with a Nishiyama–Wasserman orientation relationship to the β phase, whereas this orientation relationship was not observed in the coatings.

4. The aged melt spun materials duplicated the microstructure resulting from the commonest mode of coating $M_{23}X_6$ formation. This mode involved precipitation of $M_{23}X_6$ in association with γ′ (resulting in a cube–cube orientation relationship of β and γ′). In contrast, the melt spun foils were unable to duplicate occasional $M_{23}X_6$ precipitates present in the coatings as a result of incorporation from the substrate or precipitation in matrix phases precursoring β. No evidence was found in the melt spun materials of α-Cr or other Cr–Mo phases observed in the coatings.

References

1. T. N. RHYS-JONES, in "Materials Development in Turbo-Machinery Design", edited by D. M. R. Taplin, J. F. Knott and M. H. Lewis (Institute of Metals, London, 1989) pp. 218–223.
2. S. R. LEVINE and R. M. CAVES, *J. Electrochem Soc.* **121** (1974) 1051.
3. T. N. RHYS-JONES, *Mater. Sci. Technol.* **4** (1988) 421.
4. W. F. GALE and J. E. KING, *Metall. Trans.* **23A** (1992) 2657.
5. *Idem., J. Mater. Sci.* **28** (1993) 4347.
6. M. I. WOOD, in "Advanced Materials and Processing Techniques for Structural Applications", edited by T. Khan and A. Lasalmonie (ONERA, Chatillon, 1988) pp. 179–188.
7. T. C. TOTEMEIER, W. F. GALE and J. E. KING, *Mater. Sci. Engng* **A169** (1993) 19.
8. P. HANCOCK, H. H. CHIEN, J. R. NICHOLLS and D. J. STEPHENSON, *Surf. Coat. Technol.* **43/44** (1990) 359.
9. A. S. MURTHY and E. GOO, *Acta Metall. Mater.* **41** (1993) 3435.
10. L. E. TANNER, A. R. PELTON, G. VAN TENDELOO, D. SCHRYVERS and M. E. WALL, *Scripta Metall. Mater.* **24** (1990) 1731.
11. R. YANG, J. A. LEAKE and R. W. CAHN, *J. Mater. Res.* **6** (1991) 343.

Received 1 February 1994
and accepted 22 June 1995